International Journal of Engineering Research & Technology (IJERT)
ISSN: 2278-0181
Vol. 5 Issue 11, November-2016

A Direct Torque Control of Interior Permanent Magnet Synchronous Motor for an Electric Vehicle-Design Analysis Total Harmonic Distortion of Stator Current

Mr. Rajeev Singh [1],
[1] Post Graduate Student,
Department of EX,
TIT Bhopal, RGPV. Bhopal,
Madhya Pradesh, India

Prof. Kaushal Pratap Sengar[2],
[2]Associat Professor,
Department of EX,
TIT Bhopal, RGPV Bhopal,
Madhya Pradesh, India

Dr. Anuprita Mishra[3],
[3]H.O.D,
Department of EX, TIT
Bhopal, RGPV Bhopal,
Madhya Pradesh, India

Prof. Chitra Thakur[4],
[4]Asst. Professor,
Department of EX,
TIT Bhopal, RGPV Bhopal,
Madhya Pradesh, India

***Abstract* – Comparative studies on several direct torque control (DTC) strategies of interior permanent magnet synchronous motor (IPMSM) for electric vehicles (EVs) are discussed in details, namely basic DTC, DTC combined with space vector modulation (DTC-SVM), and dead beat DTC (DB-DTC). These DTC strategies are reviewed; meanwhile dynamics and steady-state performance are analyzed and compared. Simulations of a 20kW IPMSM for EVs are carried out for comparison studies including: ripple of torque and stator flux, sensitivity to machine's parameter, computational complexity, and total harmonic distortion**

***Keywords: Direct torque control, flux, interior permanent magnet synchronous motor, electric vehicle, deadbeat, observer, simulation*.**

1 INTRODUCTION

Electric vehicles have many advantages such as high energy efficiency, no harmful gas emissions. In recent years, with the constant improvement of the permanent magnet material per for- manse, the rapid development of power electronic components and the gradual maturation of the control algorithms, the electric car of using PMSM as power core becomes an inevitable trend.

To design a motor for electric vehicle, we must consider the special environment and application of the motor. Firstly, the mo- tor should have large starting torque and superior constant power output characteristics over a wide speed range. Secondly, the car has relatively limited space for installing a motor. The motor with built-in permanent magnet has advantages of high efficiency, small size and superior flux-weakening capability, which makes it an ideal choice for electric vehicle design

With the increasing demand of living comfort, automobile gets more and more utilized for individual and public transportation because of its convenience. But, accompanying vast fuel consumption and environmental pollution become more serious. Automobile companies focus on electric vehicles (EVs), hybrid electric vehicles (HEVs), plug-in hybrid electric vehicles (PHEVs), and fuel-cell vehicles. Among these, electric vehicles get the most attraction in recent years for its only convenient and rechargeable battery power supply and simple driver control structure. Interior permanent magnet synchronous motor (IPMSM) has some merits of high power density, high efficiency, good reliability, low torque ripple and wide range of speed regulation, which make it much fitter for electric vehicles driving than other general electric machines such as induction motor (IM), brushless DC motor (BLDC), and switch reluctance motor (SR) To promote performance of IPMSM, current vector control (CVC) is the most widely used approach to regulate the torque of IPMSM. When using CVC, stator current, rather than torque and stator flux, is the closed-loop controlled variable. In CVC of IPMSM, voltage space vectors of the inverter are the only input for closed-loop control of stator current. The stator current dynamics will affect torque and stator flux performance. For EVs, IPMSM driver will receive torque command from car controller with different operating mode. The torque precisely controlled or not, will affect car dynamics and human comfort. Therefore, the torque open-loop control of CVC is not extremely suitable for IPMSM control of EVs. Direct torque control (DTC) has closed-loop control both of torque and stator flux. At present, DTC has become a powerful and widely used control strategy of AC machines. The q axis vector decoupling of field oriented control (FOC) is replaced by two hysteresis controllers of DTC, which meets very well with the on-off operation of power transistors of inverter. DTC has some virtues of both control strategy framework and driver materials. Comparing with FOC, DTC does not require any coordinate transformation and space vector modulation. Furthermore, DTC also does not require rotator position sensor which is essential for FOC. DTC is natively sensor less leading to simplified implementation and lower

International Journal of Engineering Research & Technology (IJERT)
ISSN: 2278-0181
Vol. 5 Issue 11, November-2016

cost. DTC has comparable steady and dynamic torque performance with FOC. Additionally, DTC has low sensitivity to parameters vibration of electric machine. But, the disadvantages of basic DTC is also obvious: torque and flux ripple, deteriorated performance at low speed, and variable switching frequency of inverter. For the defects of basic DTC, much works have been made over the past few decades. DTC combined with space vector modulation (DTC-SVM) for IPMSM, is to achieve constant switching frequency of inverter as well as to obtain the desired torque and stator flux with little ripple by synthesizing an appropriate voltage space vector through SVM, which is more accurate than that of basic DTC to compensate the error of desired and actual stator flux.

In this paper, basic DTC, DTC-SVM and DB-DTC will be comparatively evaluated through simulations with various criteria. The comparison results will be used as guidance for application of IPMSM to industry and electric vehicles.

Interior Magnet Type (Ipmsm):
In this type the motor, the magnets are place inside the rotor which is shown in fig.1.3.In this Configuration Saliency is available and the air gap of d-axis is greater compare with the q axis gap Resulting that the q axis Inductance has a different value than the d axis inductance. There is inductance Variation for this type of
Rotor because the permanent magnet part is equivalent to air in the magnetic Circuit calculation. These Motors are considered to have saliency with q axis inductance greater than The d axis inductance (Lq>Ld). Due to saliency IPMSM is a good candidate for high-speed operation Such as PCB manufacturing, spindle Drives and hybrid electric vehicles (HEV) etc. Further, among Interior Permanent Magnet Synchronous Motor (IPMSM) and Surface Mounted Permanent Magnet Synchronous Motor (SMPMSM), IPMSM is preferably used for many applications due to its Constructional features along with higher demagnetizing Effect to enhance the speed above the base Speed. Although IPMSM demand gradually increasing in Various industrial applications with veracious Speed control and fast dynamic response, there still exist a Great challenge to control its speed more accurately under various conditions.

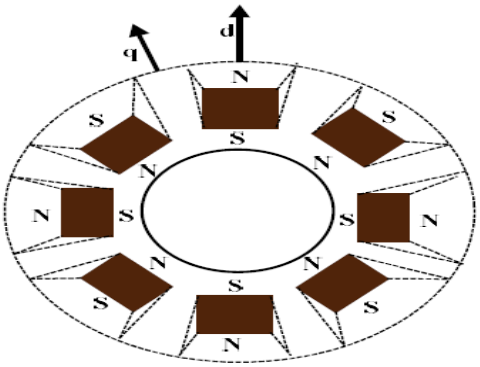

Fig.1.3 Interior PM (IP) Synchronous Machine

Vector control (or Field Oriented Control) principle makes the analysis and control of Permanent Magnet
Synchronous Motor (PMSM) drives system simpler and provides better dynamic response. It is also widely Applied in many areas where servo- like high Performance plays a secondary role to Reliability and energy Savings. To achieve the field-oriented control of PMSM, knowledge of the rotor Position is required. Usually the rotor position is measured by a shaft encoder, resolver, or hall sensors

OVERVIEW AND DYNAMIC MODELING OF IPM DRIVE SYSTEM

This chapter deals with the description and design of dynamic mathematical model of the permanent Magnet synchronous motors drive system for its vector control analysis before proceeding to design Control observation algorithms for them.

2.1. Permanent Magnet Synchronous Motor Drive System:
The motor drive consists of four main components, the PM motor, inverter, control unit and the Position Sensor. The components are connected as shown in Fig.2.1: Schematic Block diagram for Drive System

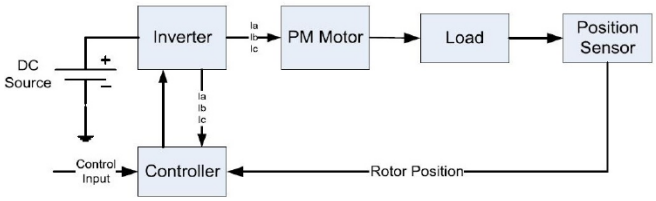

Fig.2.1: Schematic Block diagram for Drive System

2.2. Mathematical Model of IPMSM:
The mathematical model for the vector control of the PMSM can be derived from its dynamic d-q Model which can be obtained from well-known model of the induction machine with the equation of Damper winding and field current dynamics removed. The synchronously rotating rotor reference Frame is chosen so the stator winding quantities are transformed to the synchronously rotating Reference frame that is revolving at rotor speed.

The model of PMSM without damper winding has been developed on rotor reference frame using the

Following assumptions:

1. Saturation is neglected.
2. The induced EMF is sinusoidal.
3. Core losses are negligible.
4. There are no field current dynamics.

It is also be assumed that rotor flux is constant at a given operating point and concentrated along the d Axis while there is zero flux along the q axis, an assumption similarly made in the derivation of indirect Vector controlled induction motor drives .The rotor reference frame is chosen because the position of The rotor magnets determine independently of the stator voltages and currents, the instantaneous Induced Emf

International Journal of Engineering Research & Technology (IJERT)
ISSN: 2278-0181
Vol. 5 Issue 11, November-2016

and subsequently the stator currents and torque of the machine. When rotor references Frame are Considered, it means the equivalent q and d axis stator windings are transformed to the Reference frames That is revolving at rotor speed. The consequences is that there is zero speed Differential between the Rotor and stator magnetic fields and the stator q and d axis windings have a fixed phase relationship with The rotor Magnet axis which is the d axis in the modeling. The stator Equations of the induction machine in The Rotor Reference frames using flux linkages are taken to derive the model of the IPMSM as shown in Fig.

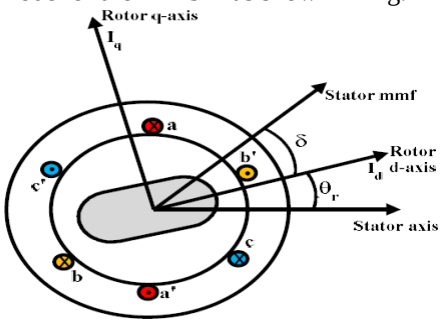

DTC is realized on base of IPMSM model. Expressions of IPMSM in rotating *dq* reference frame are listed as Follows

$$U_d = R_s i_d + \frac{d\Lambda_d}{dt} - W_e \Lambda_q$$

$$u_q = R_s i_d + \frac{d\Lambda_q}{dt} - W_e \Lambda_d$$

$$\Lambda_d = L_d i_d + \Lambda_{PM}$$

$$\Lambda_q = L_q i_q$$

(2) Where U_{dq} and I_{dq} are stator voltage and current; R_s is stator resistance; L_d and L_q are d-axis and q-axis stator inductance, respectively; Λ_{dq} *is* stator flux; W_e is electrical rotor angular velocity; Λ_{PM} is permanent magnet flux. The torque of IPMSM is

$$T_e = 1.5p\,(\Lambda_d i_q - \Lambda_q i_d) \qquad (3)$$

Where *p* is the number of rotator pole pairs.

3. BASIC DTC

3.1 DTC STRATEGY:- Basic DTC For AC machines, the torque is proportional to vector product of stator flux Λ_s and rotator flux Λ_r . For IPMSM, rotator flux is induced by permanent magnet, then $\Lambda_r = \Lambda_{PM}$, which is almost a constant. The angle velocity of rotator varies little when voltage space vector affects on stator windings during one sample period, so the torque is only decided by stator flux vector. By applying appropriate voltage space vector, basic DTC can control the magnitude and angle of stator flux to obtain desired torque. The framework of basic DTC is shown in Fig.1.

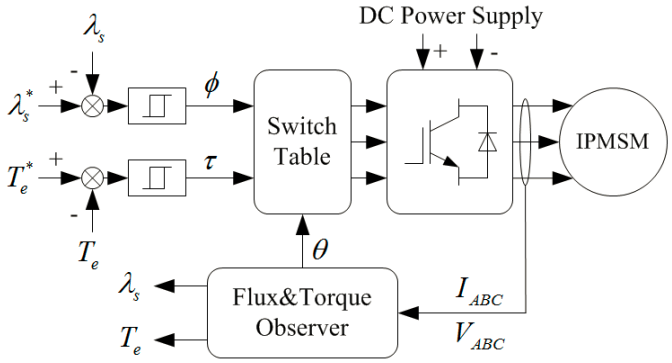

Fig.1 Framework of basic DTC.

IPMSM stator winding currents are measured by hall current sensors, and its voltages are calculated by inverter switch state. The actual stator flux and torque are calculated by flux and torque observer. The actual stator flux and torque are compared with the reference values in two separate hysteresis controllers. The hysteresis controllers are two-level comparator whose outputs are labeled with φ and T. If the actual value is less than down bounds of the reference value, the comparator outputs true (also 1) meaning that the selected voltage space vector should increase the actual value. On the other side, if the actual value is larger than up bounds of the reference value, the comparator outputs false (also 0) meaning that the selected voltage space vector should decrease the actual value. According to the outputs of two hysteresis controllers and the stator flux position, an optimal voltage space vector will be selected and applied to stator windings to minimize the error of stator flux and torque in each control period. The selection of optimal voltage space vector is referred to Table 1. In this table, θ is the section of stator flux position.

Table 1. Switch table of basic DTC

φ	T	θ					
		1	*2*	*3*	*4*	*5*	*6*
1	1	U_6	U_2	U_3	U_1	U_5	U_4
	0	U_5	U_4	U_6	U_2	U_3	U_1
0	1	U_2	U_3	U_1	U_5	U_4	U_6
	0	U_1	U_5	U_4	U_6	U_2	U_3

The parameters of IPMSM are listed in Table 2. The performance of basic DTC is shown in Fig.2. The bound of torque hysteresis control is 5N.m, and that of stator flux is 0.05Wb. Fig.2 demonstrates torque and stator flux are limited within bounds of the two separate hysteresis controllers. The ripple of torque and stator flux is controllable. The dynamic response with step-up torque reference is about 0.15ms.

International Journal of Engineering Research & Technology (IJERT)
ISSN: 2278-0181
Vol. 5 Issue 11, November-2016

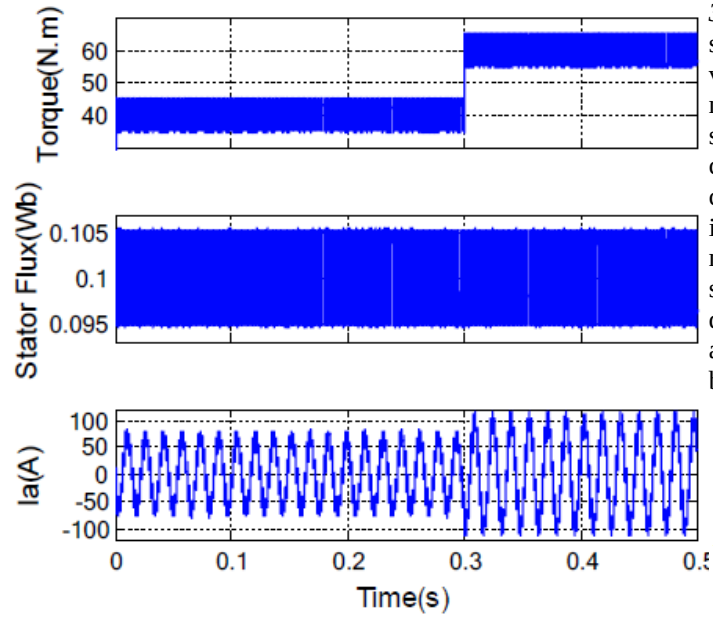

(a)

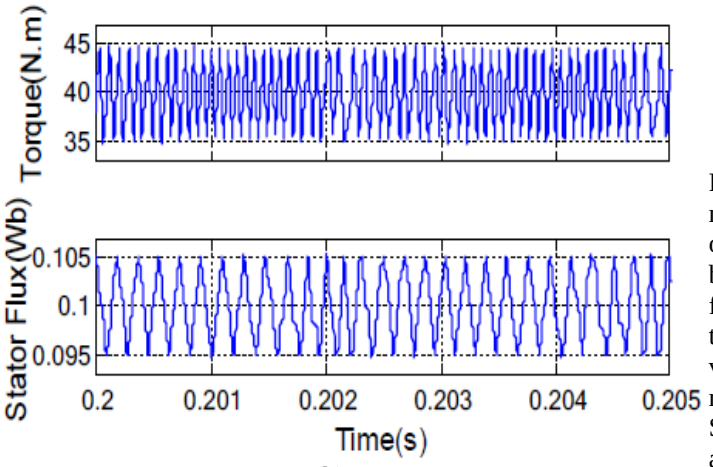

(b)

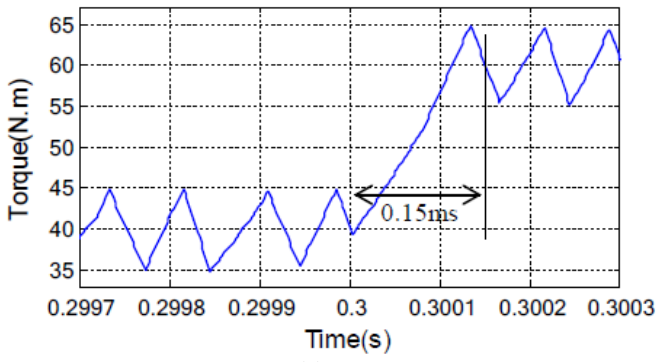

(c)

Fig. 2. Dynamic and steady performance of basic DTC. Mechanical angle velocity: 100rad/s; torque reference value: original 40N.m, step up to 60N.m at 0.3s; stator flux reference value: 0.1Wb. (a) Performance of IPMSM; (b) Amplification; (c) Dynamics of torque.

3.2 DTC-SVM For basic DTC, one of the only eight voltage space vectors (six non-zero and two zero voltage space vectors) can be selected and applied to stator windings to minimize the error of reference and actual of torque and stator flux. But, the magnitude of voltage space vector is constant, and it will activate within one whole control period continuously. Therefore, the ripple of torque and stator flux is inevitable. In order to recede the ripple of torque and flux, a more accurate voltage space vector should be applied to stator windings. Based on space vector synthesis, an arbitrary desired voltage space vector can be synthesized by two adjacent non-zero and one zero voltage space vectors. The block diagram of DTC-SVM is shown in Fig. 3.

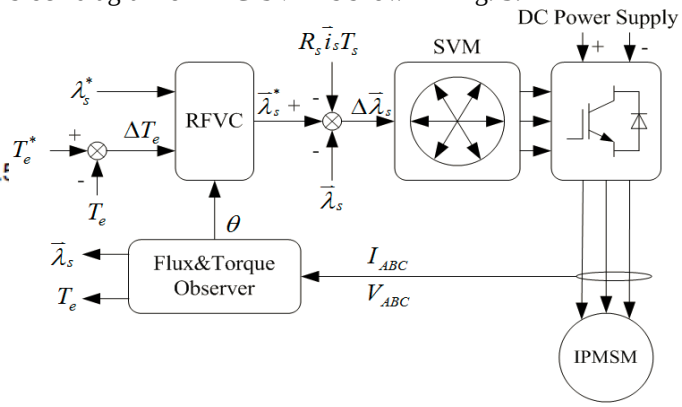

Fig. 3. Block diagram of DTC-SVM.

Reference flux vector calculator (RFVC) and space vector modulator (SVM) substitute for the two hysteresis controllers of basic DTC. Flux and torque observer is just same as that of basic DTC. Because of the torque's non-linearity to stator flux angle position, a PI regulator is used for torque variation to stator flux angle position variation. The reference flux vector calculator is just shown in Fig.4. Block diagram of reference flux vector calculator. The performance of DTC-SVM is shown in Fig.5. The ripple of torque is about 1.7N.m and the stator flux is nearly reference value with little error. The steady-state performance of torque and stator flux is much better than that of basic DTC. The dynamic response is about 0.25ms, much longer than basic DTC, which is mainly caused by PI regulator existing in RFVC

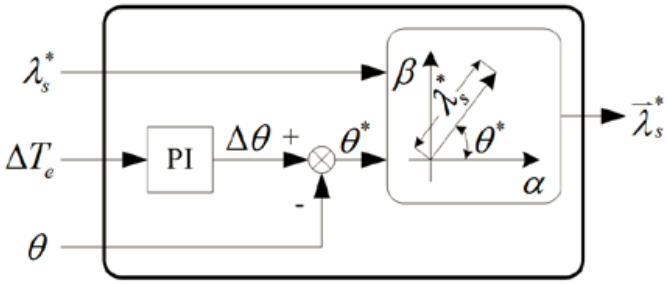

Fig. 4. Block diagram of reference flux vector calculator.

The performance of DTC-SVM is shown in Fig.5. The ripple of torque is about 1.7N.m and the stator flux is nearly reference value with little error. The steady-state performance of torque and stator flux is much better than that of basic DTC. The dynamic response is about 0.25ms, much longer than basic DTC, which is mainly caused by PI regulator existing in RFVC.

International Journal of Engineering Research & Technology (IJERT)
ISSN: 2278-0181
Vol. 5 Issue 11, November-2016

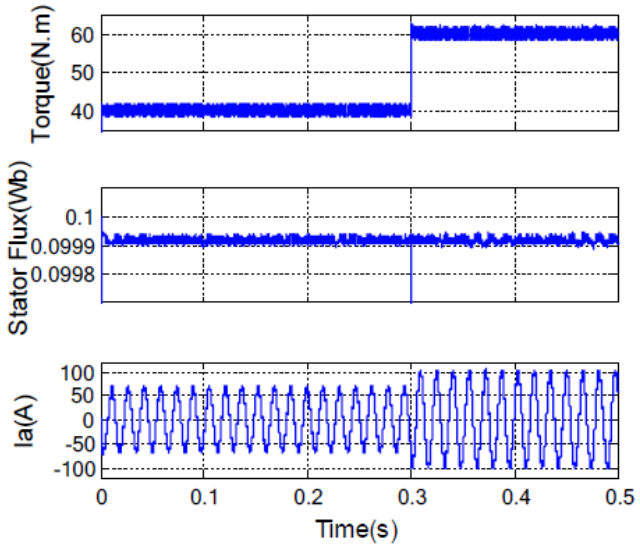

(a)

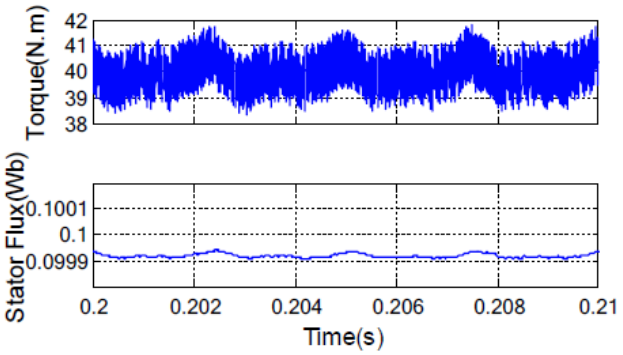

(b)

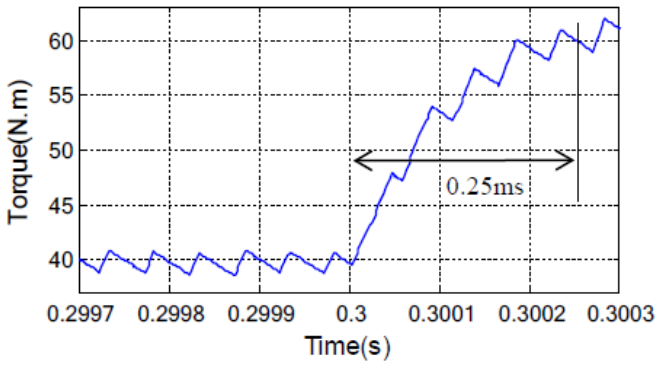

(c)

Fig. 5. Dynamic and steady performance of DTC-SVM. Mechanical angle velocity: 100rad/s; torque reference value: original 40N.m, step up to 60N.m at 0.3s; stator flux reference value: 0.1Wb. (a) Performance of IPMSM; (b) Amplification; (c) Dynamics of torque.

The torque of IPMSM is expressed as (3). Then, the corresponding differential equation is

$$\frac{dT_e}{dt} = 1.5\,p\left(\frac{d\Lambda_d}{dt}i_q + \Lambda_d\frac{di_q}{dt}i_d - \frac{d\Lambda_q}{dt}i_d - \Lambda_q\frac{di_d}{dt}\right)$$

The differential frame stator currents and stator flux of d-q reference frame are substituted into (4) from (1) and (2). Thus, the differential torque equation can be rewritten as (5),

$$\frac{dT_e}{dt} = 1.5p\left[u_d\Lambda_q\left(\frac{L_d - L_q}{L_d L_q}\right) + u_q\frac{(L_d - L_q)\Lambda_d + \Lambda_{PM}L_q}{L_d L_q} + \frac{W_e}{L_d L_q}((L_q - L_d)(\Lambda^2_d - \Lambda^2_q) - L_q\Lambda_d\Lambda_{PM}) + \frac{R_s\Lambda_q}{L^2_d L^2_q}((L^2_q - L^2_d)\Lambda_d - L^2_q\Lambda_{PM})\right] \quad (5)$$

And the discrete time form of (5) is

$$\frac{T_e(k+1) - T_e(k)}{T_s} = 1.5p\left[u_d(k)\Lambda_q(k)\left(\frac{L_d - L_q}{L_d L_q}\right) + u_q(k)\frac{(L_d - L_q)\Lambda_d(k) + \Lambda_{PM}L_q}{L_d L_q} + \frac{w_e(k)}{L^2_d L^2_q}(L^2_q - L^2_d)\Lambda_d(k) - L^2_q\Lambda_{PM})\right] \quad (6)$$

T_S in (6) is sampling period. The torque variation in (6) can be expressed as an variable ΔT_e by

$$\Delta T_e(k) = T_e(K+1) - T_e(k) \quad (7)$$

The relationship of d-q axis stator voltage can be developed from (6) including $\Delta T_e(k)$ as the desired torque change

$$u_q(k)T_s = Mu_d(k)T_s + B \quad (8)$$

Where

$$M = \frac{(L_q - L_d)\Lambda_q(k)}{(L_d - L_q)\Lambda_d(k) + L_q\Lambda_{PM}}$$

$$B = \frac{L_d L_q}{(L_d - L_q)\Lambda_d(k) + L_q\Lambda_{PM}}$$

$$\left[\frac{2\Delta T_e(k)}{3p} - \frac{W_e T_s}{L_d L_q}((L_q - L_d)(\Lambda_d(k)^2 - \Lambda_q(k)^2) - L_q\Lambda_d(k)\Lambda_{PM}) + \frac{R_s T_s\Lambda_q(k)}{L^2_d L^2_q}((L^2_q - L^2_d)\Lambda_d - L^2_q\Lambda_{PM})\right]$$

Using (8), stator voltage vectors will be calculated to achieve the desired torque variation over the next sample time, which implements deadbeat torque control. But, the stator flux will not be controlled simultaneously with the torque and vary in random. In order to achieve deadbeat flux control, the d-q axis stator flux vectors should be taken into account and imported into torque control. Then, the voltage model of stator flux is introduced as

International Journal of Engineering Research & Technology (IJERT)
ISSN: 2278-0181
Vol. 5 Issue 11, November-2016

$$\Lambda_{dq} = \int (u_{dq} - R_s i_{dq})dt \quad (9)$$

When the stator resistance is small enough to be negligible, the discrete time of stator flux vector is approximately

$$\Lambda_{dq}(k+1) = \Lambda_{dq}(k) + u_{dq}(k)\, T_s \quad (10)$$

In (10), $\Lambda_{dq}(K+1)$ is the desired stator flux, that is,

The block diagram of DB-DTC is shown in Fig.6. The flux and torque estimation with current observer is different from that of basic DTC and DTC-SVM. It contains current predictive model composed of PI regulators and current filters presented by Lee (2011). The DB-DTC controller is equations with (7), (8), (10) and (11).

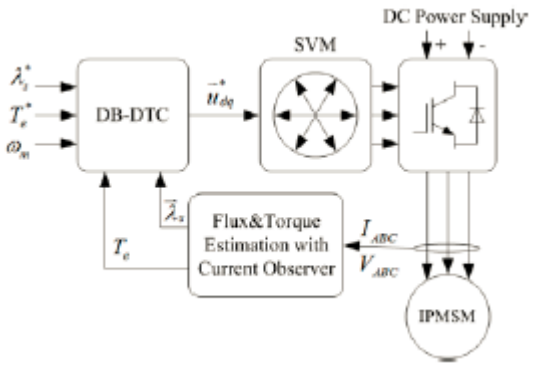

Fig. 6. Block diagram of DB-DTC.

The performance of DB-DTC is shown in Fig. 7. The torque ripple is less than 1N.m, and also less than that of DTC-SVM. But, the stator flux ripple is nearly 1%, larger than that of DTC-SVM. The dynamic response is about 0.85ms, much longer than basic DTC and DTV-SVM, mainly caused by PI regulator existing in stator flux and torque estimation.

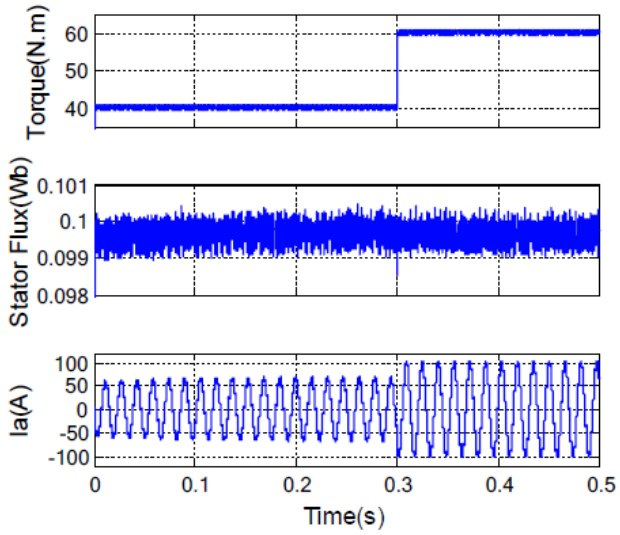

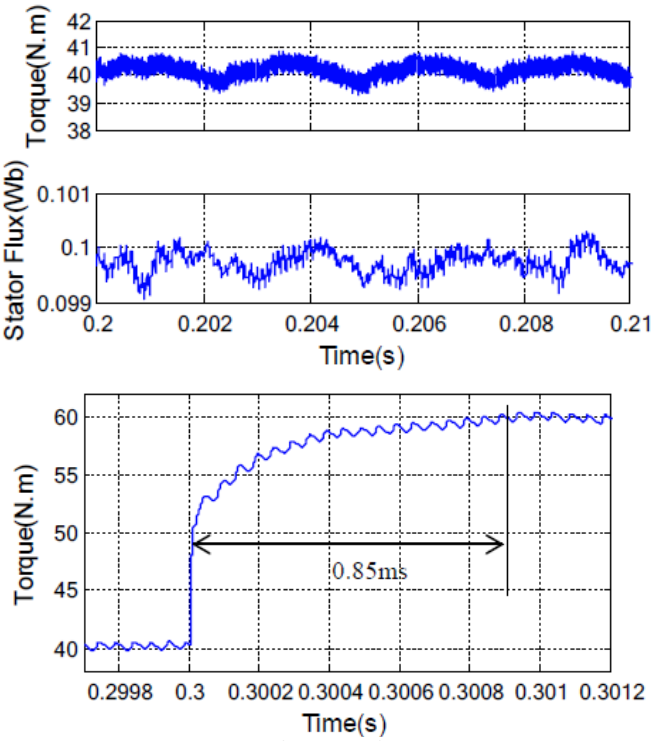

Fig. 7. Dynamic and steady performance of DB-DTC. Mechanical angle velocity: 100rad/s; torque reference value: original 40N.m, step up to 60N.m at 0.3s; stator flux reference value: 0.1Wb. (a) Performance of IPMSM; (b) Amplification; (c) Dynamics of torque.

4 PERFORMANCE EVALUATIONS

Based on the optimization results, the optimal PM brushless machine is established and the corresponding electromagnetic performance of the optimal PM brushless machine is analyzed in detail by the finite element method (FEM). Meanwhile, an EV involving the PM brushless machine is built and tested based on the urban dynamometer driving schedule (UDDS) for evaluation.

4.1. Performances Comparison over the Urban Dynamometer Driving Schedule

To further verify the validity of the proposed design and optimization method, an integrated EV model, which consists of wheel/axle, transmission, motor, and energy storage, is built. As shown in Figure 8, the motor is connected to the front axle, where the transmission and differential are assembled in a shell, thus reducing the transmission losses and improving the transmission efficiency. By the secondary development, the initial and optimal PM brushless machine is applied to the EV model respectively so that the simulation model based on Simulink can be obtained, as shown in Figure 9, where, the backward and forward simulation models are combined. That is, the driving schedule claims specific torque and speed from the vehicle, and each module demands required torque and speed from its superior module in the direction of the backward simulation data flow. When the data flow arrives at the final energy storage, the battery will supply available energy according to the requirements. Then, available torque and speed are transmitted to the junior module in the direction of the forward simulation data flow, meanwhile, the real torque and speed can also

International Journal of Engineering Research & Technology (IJERT)
ISSN: 2278-0181
Vol. 5 Issue 11, November-2016

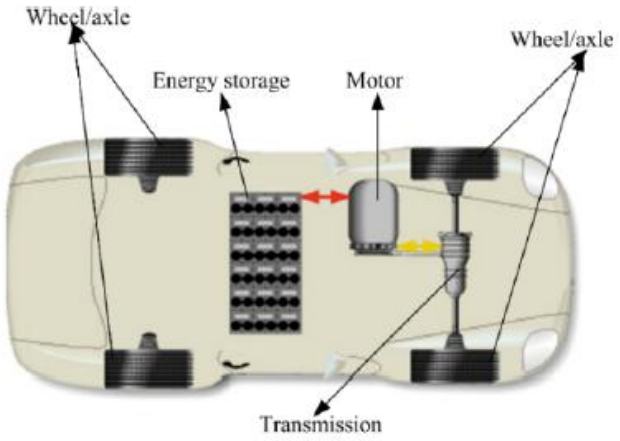

Figure 8. Integrated electric vehicle (EV) model.

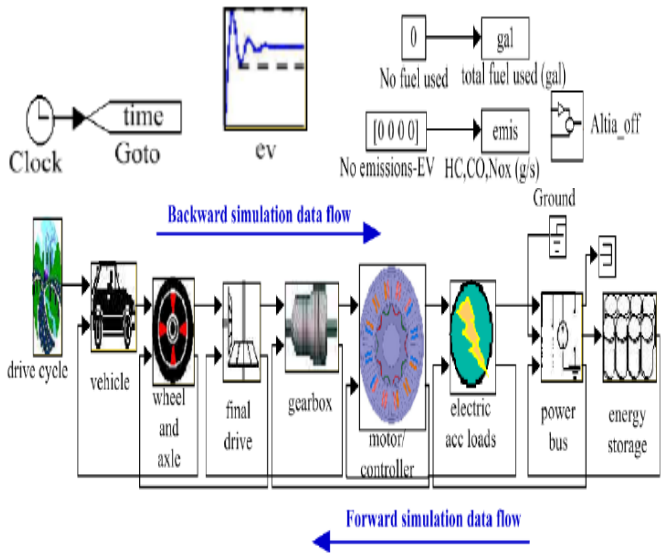

Figure 9. Simulation model of the EV involving the PM brushless machine.

Based on the efficiency map, the integrated EV models involving the initial and optimal machines are simulated and compared over the UDDS. By employing the proposed design and optimization method, the optimal PM brushless machine obtains a wider constant power speed range. Thus, compared to the EV employing the initial PM brushless machine, the EV employing the optimal one exhibits better torque and speed production ability. It can also be observed from that, the state of charge (SOC) of the energy storage decreases during the acceleration process, while the SOC increases when decelerating. Additionally, the SOC of the energy storage of the EV adopting the initial PM brushless machine shows a higher rate of change, which may bring higher requirements on the power electronic devices. Moreover, owing to the higher efficiency at high speed with low torque, the energy storage in the EV employing the PM brushless machine exhibits higher SOC. As a result, the utilization ratio of the energy storage is improved, hence saving the energy.

4.2 Parameter Sensitivity: - In various applications, IPMSM's parameters may vary with ambient temperature. The machine's parameters mainly are stator resistance, d-q axis inductance and rotator permanent magnet flux. The parameter sensitivity of control strategies will determinate the performance of IPMSM. Here, the performance of DTC strategies with variation of machine's parameters is evaluated through some simulations. Fig. 8 shows the torque ripple and flux ripple of the three different DTC strategies with the value of stator resistance exceeding the actual value by 20% and q-axis inductance by less 20%. The simulation results demonstrate that, when the q-axis inductance and stator resistance vary, the steady performance of stator flux and torque are not much deteriorated. The torque ripple gets increased a little while parameters vary. Therefore, the three DTC strategies are non-sensitive to this machine's parameters variation.

4.3 Computational Complexity:- For these three DTC strategies, the computational complexity is linear to the core algorithm. The flux and torque observer of basic DTC and DTC-SVM are identical. This observer only calculates actual values of stator flux and its angle position and torque by the measured stator currents and stator voltages deduced by switch state of inverter. But, DB-DTC's flux and torque estimation contains current observer with PI and filters, who will consume more computational time. Besides of flux and torque observer, basic DTC needs minimum time for computation that has only hysteresis comparator and voltage selection. On the other hand, DB-DTC has the maximum time for computation because of its computation complexity of reference d-q axis stator voltages. DB-DTC has the same space vector modulation as DTC-SVM for constant stator flux.

4.4 Stator Current THD:- For electric vehicle, power losses of motor and driver affect the efficiency of car electrical system, and furthermore the travel distance. The frequency spectrum of stator currents affects iron losses of motor. For AC machine, the total harmonic distortion (THD) is widely used for frequency spectrum performance. When steady, the stator currents and their THD are shown in Fig.9. The simulation is set at mechanical angle velocity of 100rad/s constantly and the desired torque of 40N.m for different DTC strategies. From Fig.9, it can be seen that basic DTC has the highest THD, while DTC-SVM and DB-DTC have almost equivalent lower THD. Correspondingly as formulations before, basic DTC has the highest torque ripple and flux ripple. The highest stator current THD of basic DTC is primarily caused by the torque ripple and flux ripple, which could be improved by decreasing the hysteresis comparator bounds and enhancing sampling and switching frequency of inverter.

International Journal of Engineering Research & Technology (IJERT)
ISSN: 2278-0181
Vol. 5 Issue 11, November-2016

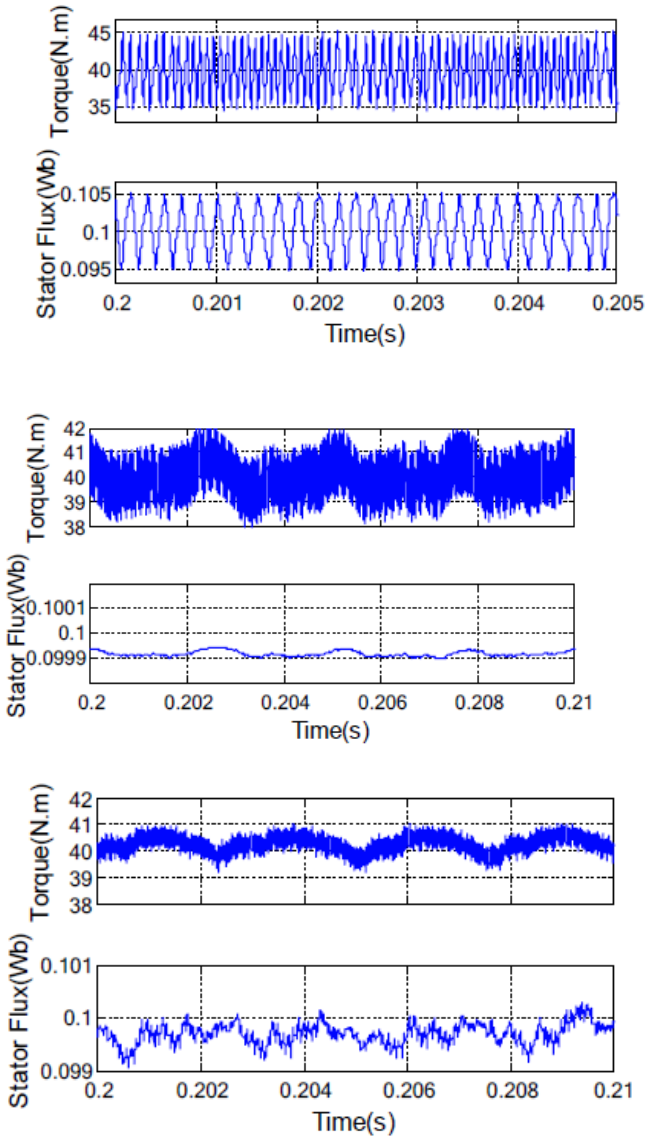

Fig. 8. Performance with variation of machine's parameters. (a) Basic DTC; (b) DTC-SVM; (c) DB-DTC

Table 2. Parameters of IPMSM

Rated power P_N (kW)	20
Rated DC voltage U_{dc} (V)	336
Rated Torque T_e (N.m)	64
Stator Resistance R_s (Ω)	0.02
Inductance of d axis L_d (mH)	0.336
Inductance of q axis L_q (mH)	0.5
Permanent Magnet Flux of Rotator λ_{PM} (Wb)	0.1
Pole pairs p	4

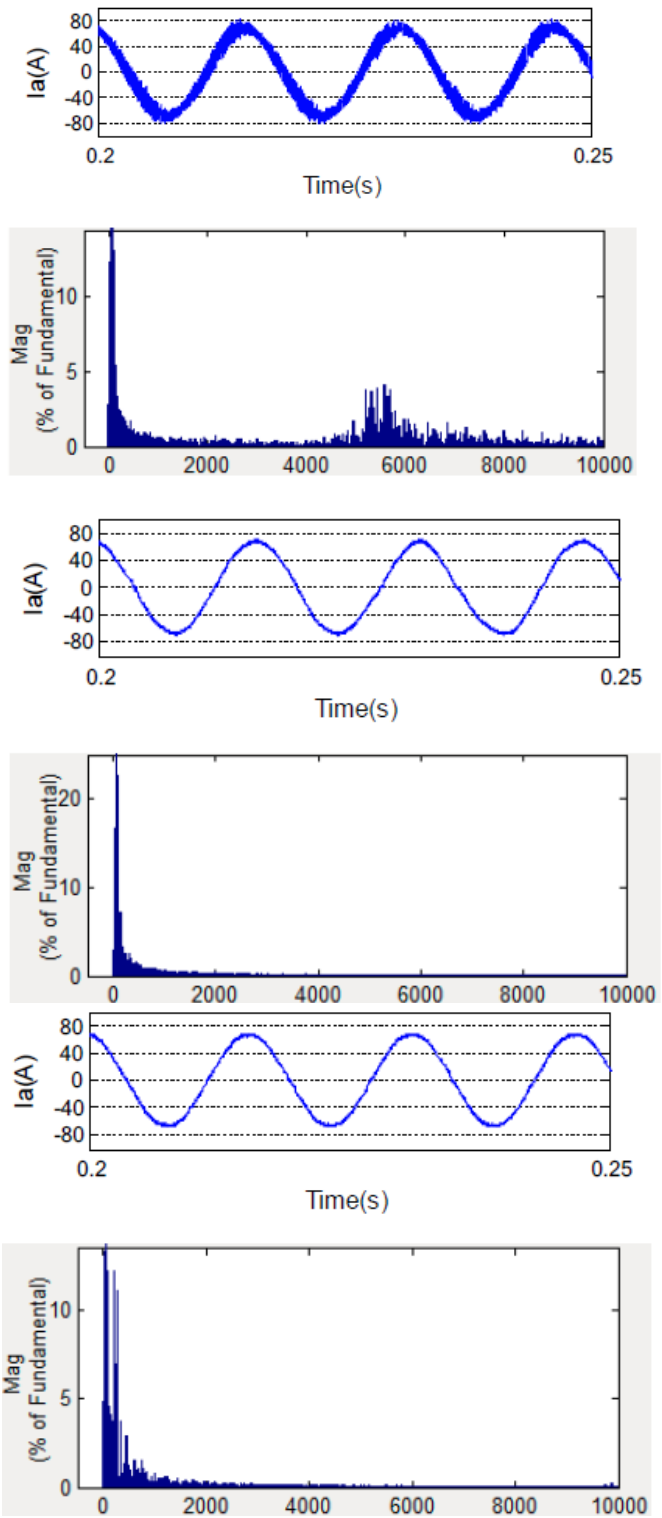

Fig. 9. THD for stator current.(a)Basic DTC: Fundamental (60Hz) = 67.37, THD= 16.63%; (b)DTC-SVM: Fundamental (60Hz) = 67.77, THD= 7.59%; (c)DB-DTC: Fundamental (60Hz) = 67.71, THD= 7.57%.

International Journal of Engineering Research & Technology (IJERT)
ISSN: 2278-0181
Vol. 5 Issue 11, November-2016

5. CONCLUSIONS

In this paper, a new design and optimization method is proposed for PM brushless machines to satisfy requirements of the multiple driving conditions in EVs. It has been shown that the proposed design method considering the maximum operating speed and performances specifications over the entire speed range is effective to give an initial PM brushless machine with well performances. Moreover, based on increasing d-axis inductance and meanwhile maintaining constant PM flux linkage, the proposed optimization method can achieve a wider constant power speed range, as well as reduced the losses and improved efficiency over the torque-speed envelope, especially in the high-speed region. Consequently, the SOC of the energy storage is increased, thus improving the energy utilization ratio. Both the analysis and simulation results reveal the feasibility of the optimal PM brushless machine to be applied in the EV, hence verifying the validity of the proposed design and optimization method for EV traction machines.

REFERENCES

[1] M. Zeraoulia, and *et al*, "Electric motor drive selection issues for HEV propulsion systems: A comparative study," *IEEE Trans. Vehicular Tech.*, vol. 55, pp.1756-1763, Nov. 2015.
[2] L. Chang, "Comparison of ac drives for electric vehicles- A report on experts' opinion survey," IEEE AES Systems Magz. pp.7-10, Aug. 1994.
[3] T. Backstrom, Integrated energy transducer drive for hybrid electric vehicles, PhD Thesis, Royal Institute of Technology, Sweden, 2000.
[4] C. Mi, "Analytical design of permanent-magnet traction-drive motors," IEEE Trans. Magn., vol. 42,pp. 1861-1866, July, 2006.
[5] Y. Fujishima, S. Vakao, M. Kondo, and N. Terauchi, "An optimal design of interior permanent magnet synchronous motor for the next generation commuter train," IEEE Trans. Applied Superconductivity, vol. 14, pp.1902-1905, June 2004.
[6] F. Magnussen, P. Thelin, and C. Sadarangani, "Design of compact permanent magnet machines for a novel HEV propulsion system," *in Proc*. 20th Int. Electric Vehicle Symposium and Exposition, Long beach,California, USA, 15-19 Nov., 2003, pp. 181-191.
[7] S. Wu, L. Song, and S. Cui, "Study on improving the performance of permanent magnet wheel motor for the electric vehicle application," IEEE Trans. Magn., vol. 43, pp. 438-442, Jan 2007.
[8] Nam K , Fujimoto H , Hori Y . Advanced motion control of electric vehicles based on robust lateral tire force control via active front steering. IEEE/ASME Trans Mechatron 2014;19(1):289–99 .
[9] Burress TA , Coomer CL , Campbell SL , et al. Evaluation of the 2008 lexus ls 600h hybrid synergy drive system. oak ridge national laboratory (ORNL). TN: Oak Ridge; 2009 .
[10] Chin Y-k , Soulard J . Modelling of iron losses in permanent magnet synchronous motos with field-weakening capability for electric vehicles. Int J Automot Tech- nol 2003;4(2):87–94 .
[11] Wang C , Xia J , Yang J . Modern control technique of electric machines. Beijing, China: China Machine PRESS; 2006 .
[12] Yanliang X . Study on power capability and flux-weakening level of perma- nent magnet synchronous motor in electric vehicle application. J Shandong Uni 2002;32(5):412–17 .
[13] Mellor PH , Wrobel R , McNeill N , et al. Impact of winding and rotor design on efficiency and torque ripple in brushless AC permanent magnet traction motors. In: Power electronics machines and drives, York; 2008 .
[14] Li C , Kou B , Cheng S . Outline for flux weakening of permanent magnet syn- chronous motor. Micro Motor 2008;1(1):58–60 .
[15] Yin S , Zhu X . Intelligent particle filter and its application on fault detection of nonlinear system. IEEE Trans Indust Electron 2015;62(6):3852–61 .
[16] Yin S , Wang G . Robust PLS approach for KPI related prediction and diagnosis against outliers and missing data. Int J Syst Sci 2014;45(7):1375–82 .
[17] Yin S , Zhu X , Kaynak O . Improved PLS focused on key performance indictor related fault diagnosis. IEEE Trans Indust Electron 2015;62(3):1651–8 .
[18] Jahns TM , Han S-H , EL-Refaie AM , Baek J-H , Soong WL . Design and experimen- tal verification of a 50 kW interior permanent magnet synchronous machine. In: Industry applications conference; 2006. p. 1941–6 .
[19] Stumberger B , Stumberger G , Jesenik M , Gorican V , Hamler A , Trlep M . Power capability and flux-weakening performance of interior permanent magnet syn- chronous motor with multiple flux barriers. In: 12th Biennial IEEE conference on electromagnetic field computation; 2006. p. 419 .
[20] Kwak S-Y , Kim J-K , Jung H-K . Characteristic analysis of multilayer-buried mag- net synchronous motor using fixed permeability method. IEEE Trans Energy Convers 2005;20(3):549–55 .
[21] Silva LI , Bouscayrol A , De Angelo CH , et al. Coupling bond graph and en- ergetic macroscopic representation for electric vehicle simulation. Mechatron 2014;24(7):906–13 .
[22] Ma L., Sanada M., Morimoto S., Takeda Y., "Prediction of iron loss in rotating machines with rotational lossincluded", IEEE Transactions on Magnetics, 39(4), pp. 2036 ~ 2041, 2003.
[23] Morimoto S., Takeda Y., Hirasa T., Taniguchi K., "Expansion of operating limits for permanent magnet motor by current vector control considering inverter capacity", IEEE Transactions on Industrial Applications, 26, pp. 886 ~ 871, 1990.
[24] Rabinovici R., "Eddy current losses of permanent magnet motors", IEEE Proceedings of Electric Power Application, 141(1), 1994.
[25] Say M.G., *The Performance and Design of Alternating Current Machines*,Pitman, Third Edition, SBN: 273-40199-8, 1958.
[26] Schiferl R.F., Lipo T.A., "Power capability of salient pole permanent magnet synchronous motor in variable speed drive applications", IEEE Transactions on Industrial Applications, 26, pp. 115 ~ 123, 1990.
[27] Sebastian T., Slemon G.R., "Operating limits inverter-driven permanent magnet motor drives", IEEE Transaction on Industrial Applications, 23, pp. 327 ~ 333, 1987.